IL NUOVO CIMENTO **40 C** (2017) 112
DOI 10.1393/ncc/i2017-17112-8

COLLOQUIA: SciNeGHE 2016

A new measurement of cosmic-ray electrons with the *Fermi* Large Area Telescope

A. MANFREDA(1)(2) for the *Fermi* LAT COLLABORATION

(1) *INFN, Sezione di Pisa - Pisa, Italy*
(2) *Università di Pisa - Pisa, Italy*

received 3 June 2017

Summary. — I present an updated measurement of the cosmic-ray electron and positron spectrum between 7 GeV and 2 TeV, based on 7 years of data collected with the *Fermi* Large Area Telescope (LAT). The LAT is the first space-based instrument to directly explore the region above 1 TeV. The best fit to the spectrum that we measure is given by a broken power-law, with the break located at ~ 50 GeV. Above 50 GeV our data are well described by a single power-law with a spectral index of 3.07 ± 0.02 (stat + syst) ± 0.04 (energy scale). An exponential cutoff lower than 1.8 TeV is excluded at 95% CL.

1. – Introduction

High-energy cosmic-ray electrons and positrons (CREs) constitute a peculiar component of the cosmic radiation. In fact, unlike protons and heavier nuclei, they rapidly lose energy by synchrotron radiation on galactic magnetic fields and by inverse Compton scattering on the interstellar radiation field. At ~ 1 TeV, the diffusion distance of CREs is of the order of a few hundred parsecs, much shorter than the radius of our Galaxy [1]; thus, measuring the CRE spectrum up to a few TeV can provide evidence of local CRE sources from astrophysical origin (supernova remnants and pulsar wind nebulae [2-7]) or from exotic origin (dark matter [8-10]) and constrain theoretical models of propagation of CRs in the nearby or local galactic space.

Here I present a measurement of the CRE spectrum from 7 GeV to 2 TeV based on the data collected by the Large Area Telscope (LAT) on the *Fermi* mission between August 4, 2008 and June 24, 2015. A publication describing the work in full detail was in preparation at the time this document was being written and is now published in [11].

The LAT [12] is a pair conversion telescope, designed for measuring γ rays in an energy range from a few tens of MeV to a few hundreds of GeV. It is composed of three main subsystems: a silicon tracker (TKR), for measuring the direction of incident particles; a CsI(Tl) calorimeter (CAL), located below the TKR, for energy measurement; a

segmented anti-coincidence detector (ACD) for charged cosmic-ray background rejection. Since electromagnetic cascades are common to both electron and photon interactions in matter, the LAT is also by its nature a detector for electrons and positrons. Measurements of the inclusive CRE spectrum up to 1 TeV have been published by the LAT Collaboration in 2009 [13] and 2010 [14], based on six months and one year of data, respectively.

Recently, the *Fermi* LAT Collaboration has released a radical revision of the entire event analysis, going under the name of Pass 8 [15]. Pass 8 came with improvements in all the main areas of the analysis, including Monte Carlo simulation of the detector, track and shower reconstruction, background rejection and control of the systematic uncertainties. Thanks to Pass 8, as well as to the increased statistics, we were able to extend the upper energy limit of the measurement to 2 TeV. We also seized the opportunity to refine our estimate of the systematic uncertainties and to further investigate the effects of the geomagnetic field on the low-energy end of the spectrum, as described in detail in sect. **3**. For all these reasons, the work presented here should be regarded not merely as an update of our previous measurements, but as an effectively new one.

2. – Event selection

The LAT is equipped with an on-board filter, designed to reject charged particles and reduce the data flow to a level compatible with the available telemetry bandwidth. However, the filter accepts by default all the events that deposit at least 20 GeV in the calorimeter, a condition which is typically satisfied by CREs above 40 GeV. Below that energy, it is possible to extend the measurement by using an unbiased sample of all the instrument triggers, pre-scaled by a factor 250, which is provided on the LAT mostly for diagnostic purposes. Thus, two independent event selections have been developed: *Low Energy* (LE), from 7 GeV to 70 GeV, using events from the unbiased trigger sample; *High Energy* (HE), above 42 GeV, using events from the standard on-board filter. The region of overlap is useful for cross-checking the two analyses.

We select particles with a successfully reconstructed track, a direction within 60° from the instrument boresight and which cross at least 8 radiation length of material in the CAL. We also impose minimal cuts on the quality of energy and direction measurement, in order to get rid of poorly reconstructed events. We exploit the dependence of ionization on Z^2 (where Z is the atomic number of the bullet) to easily tag and remove particles with $Z > 1$ from the dataset, cutting on the amount of ionization produced in the TKR and in the ACD.

Discrimination between protons and electrons is based on the different topology of hadronic and leptonic events in the detector. For the task, we made use of machine-learning algorithms, namely Boosted Decision Trees (BDTs), which are able to combine the information carried by several different individual observables into a single variable, P_{CRE}, which can then be used to select signal events. BDTs were trained on simulated Monte Carlo (MC) samples of electrons and protons interacting in the LAT. We trained different BDTs in different energy ranges to account for the changes in event topology in the LAT; 8 BDTs were trained for the HE analysis, and one for the LE analysis.

As shown in fig. 1, we estimate the residual background contamination by fitting, in each energy bin, the distribution of P_{CRE} in data with the sum of the MC templates for electrons and protons, letting their normalization float as free parameters for the fit. We use the renormalized MC proton template to estimate the number of background events surviving the selection, which are then subtracted from data counts to obtain the

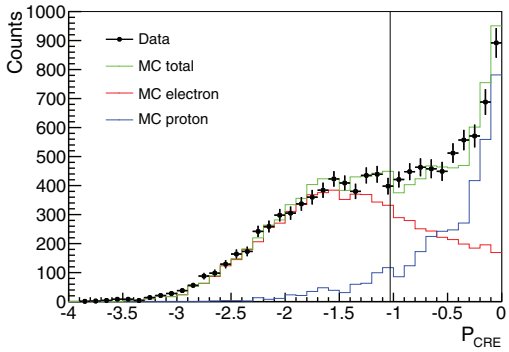

Fig. 1. – Distribution of the CRE estimator $P_{\rm CRE}$ for events between 866 and 1000 GeV. The MC prediction (green) is the sum of the signal (red) and background (blue) templates scaled by the normalization factors given by the template fit to flight-data (black). The selection cut for this energy bin is indicated by the black vertical line.

number of signal CRE events.

The acceptance and the estimated residual background contamination for the HE and LE selection are shown in fig. 2

3. – LE orbital selections

Below $\sim$ 20 GeV, the spectrum of CREs observed by the LAT is strongly influenced by the shielding effect of the magnetic field of the Earth. At a given geomagnetic position, only Galactic charged particles above a certain rigidity (which depends on their direction respect to the local zenith) can reach the detector. The orbit of *Fermi* spans an interval of vertical rigidity cut-off values from $\sim$ 6 GeV to $\sim$ 14 GeV; in order to meaure the CRE spectrum in this energy range we selected only data collected in orbital regions in which the entire bin was above the local rigidity cutoff. For the selection, we use the McIlwain L parameter [16] to conveniently parametrize the dependence of the rigidity

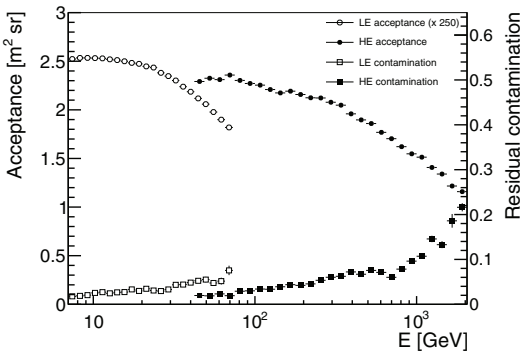

Fig. 2. – Acceptance and residual background contamination for the LE and HE selections. The displayed LE acceptance is multiplied by 250 (as if there were no prescale factor due to the on-board filter). For the acceptance, the energy is the true energy, while it is the measured energy for the contamination.

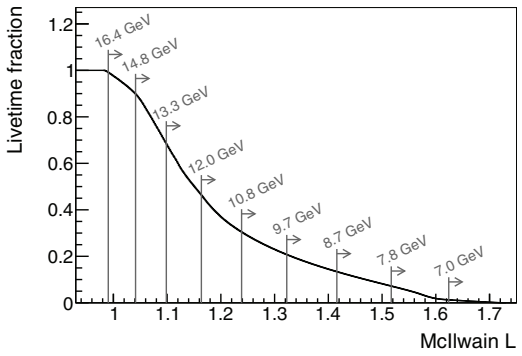

Fig. 3. – Normalized integral distribution of the instrument live time in different McIlwain L bins for the data sample. Grey lines show the McIlwain L cut in each energy bin (with numbers indicating the lower edge of the bin).

cut-off on geographic coordinates. The corresponding fraction of live time spent by the LAT in the selected regions is shown in fig. 3.

The cutoff is smooth and even above the nominal rigidity cutoff there is still a fraction of electrons and positrons which are prevented from reaching the detector by the magnetic shadow of the Earth. The effect is enhanced by a combination of the wide angular aperture of the LAT and its periodic rocking motion with respect to the local zenith, causing the Earth to be often very close to the edge of the instrument's field of view.

In order to estimate this fraction of undetected CREs and to correct the observed flux accordingly, we developed a realistic simulation of the trajectories of electrons and positrons in the orbital environment of the LAT. We use the particle trajectory tracing code developed by Smart and Shea [16] and the 2010 model of the Earth's magnetic field from the International Geomagnetic Reference Field (IGRF) [17], as we did in [18]. For a given McIlwain L selection, we use the output of the simulation to estimate the fraction of trajectories blocked by the magnetic shield of the Earth, corresponding in the real world to the fraction of unobserved CREs. The correction factors found are shown in fig. 4.

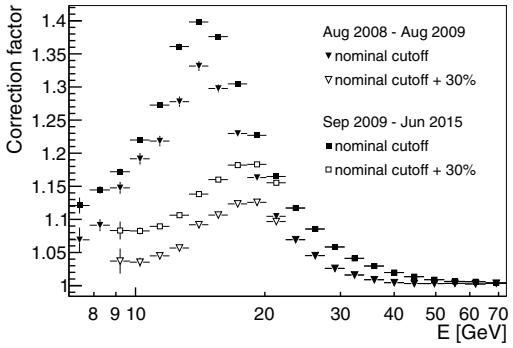

Fig. 4. – LE correction factors for the first year of the mission (triangles) and for the following years (squares). Full markers correspond to the nominal energy cutoff, while the empty markers correspond to a cutoff 30% higher.

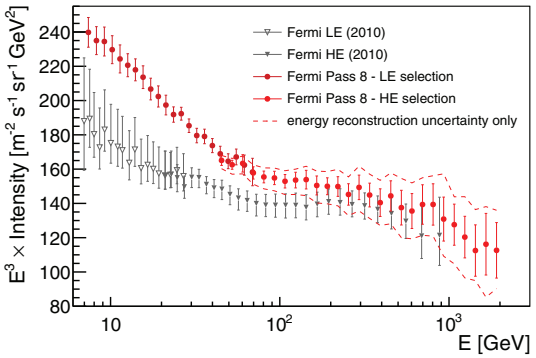

Fig. 5. – CRE spectrum between 7 GeV and 2 TeV measured by the LAT and the previous LAT measurement [14]. All error bars represent the quadratic sum of statistical and systematic uncertainties (except the one on the energy measurement). The area between the dashed lines corresponds to the uncertainty band due to the LAT energy reconstruction uncertainty only. A further 2% systematic uncertainty on the energy scale is not indicated in the plot.

We note that this effect was not explicitly accounted for in our previous measurements, though it was mitigated by the fact that the rocking angle of the instrument was smaller during the first year of the mission (it has been increased from 35° to 50° since then).

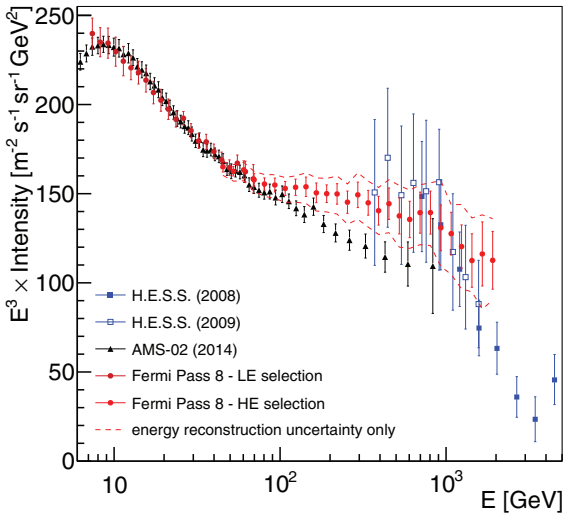

Fig. 6. – CRE spectrum between 7 GeV and 2 TeV measured by the LAT along with other recent measurements by AMS-02 [20] and H.E.S.S. [21,22]. All error bars represent the quadratic sum of statistical and systematic uncertainties (except the one on the energy measurement). The area between the dashed lines corresponds to the uncertainty band due to the LAT energy measurement uncertainty only. A further 2% systematic uncertainty on the energy scale is not indicated in the plot.

4. – Results

Here I briefly report the most relevant results of this work. A longer discussion is given in [11], including a detailed description of the techniques used to estimate the systematic uncertainties and how they were accounted for when fitting the data. We note that, at the end of the selection, the data sample contains more than 10^7 events, nearly 10^4 of which above 1 TeV; consequently, the analysis is limited by systematic uncertainties across the whole energy range.

Figure 5 shows the spectra we measured with the LE and HE analysis. We note that the two spectra match very well over the overlapping range $42 < E < 70\,\text{GeV}$. Below 100 GeV, the new LAT measurement differs from the previous one by 10–30%. A large part of this difference below 30 GeV is due to the lack of correction in the previous analysis for the loss of CREs above the geomagnetic energy cutoff. After applying this correction, the remaining difference is 10–15% and is due to imperfections in the simulation that was used in the previous analysis (remnants of electronic signals from out-of-time particles were not simulated [19]).

Figure 5 suggests the presence of a break in the spectrum. Indeed, a broken power-law fit to our data is preferred over a single power-law at the 4σ level. Fitting with a broken power-law yields a break energy of $53 \pm 8\,\text{GeV}$ and the spectral indices below and above the break are 3.21 ± 0.02 and 3.07 ± 0.02, respectively.

Figure 6 shows a comparison of the spectrum with other recent measurements from AMS-02 [20] and H.E.S.S. [21,22]. As can be seen, the LAT CRE spectrum is consistently above the AMS-02 one for energies larger than $\sim 70\,\text{GeV}$. The difference in spectral indices above 30.2 GeV, limit above which AMS-02 reports a single power-law spectrum, is at the level of 1.7σ. This could indicate that systematic uncertainties on the energy measurement in one or both of the results are slightly larger than estimated.

At higher energies, H.E.S.S. reported in [21] that its data were well reproduced by an exponentially cutoff power-law with a cutoff at $2.1 \pm 0.3\,\text{TeV}$. The LAT CRE spectrum above 50 GeV, as indicated by the previous broken power-law fits, is compatible with a single power-law with a spectral index of 3.07 ± 0.02 (stat+syst) ± 0.04 (energy measurement). Fitting the count spectrum above 50 GeV with an exponentially cutoff power-law $E^{-\gamma} e^{-E/E_c}$ does not yield statistically significant evidence for a cutoff and we exclude $E_c < 1.8\,\text{TeV}$ at 95% CL.

REFERENCES

[1] Nishimura J., Fujii M. and Taira T., in *Proceedings of the 16th International Cosmic Ray Conference*, Vol. **1** (Tokyo Univ. Inst. Cosm. Ray Res.) 1980, p. 488.
[2] Shen C. S., *Astrophys. J.*, **162** (1970) L181.
[3] Nishimura J. *et al.*, *Astrophys. J.*, **238** (1980) 394.
[4] Nishimura J., Kobayashi T., Komori Y. and Yoshida K., *Adv. Space Res.*, **19** (1997) 767.
[5] Aharonian F. A., Atoyan A. M. and Voelk H. J., *Astron. Astrophys.*, **294** (1995) L41.
[6] Kobayashi T., Komori Y., Yoshida K. and Nishimura J., *Astrophys. J.*, **601** (2004) 340.
[7] Blasi P., *Phys. Rev. Lett.*, **103** (2009) 051104.
[8] Cholis I., Goodenough L., Hooper D., Simet M. and Weiner N., *Phys. Rev. D*, **80** (2009) 123511.
[9] Cirelli M., Kadastik M., Raidal M. and Strumia A., *Nucl. Phys. B*, **813** (2009) 1; **873** (2013) 530.

[10] Bergstrom L., Edsjo J. and Zaharijas G., *Phys. Rev. Lett.*, **103** (2009) 031103.
[11] Fermi LAT Collaboration (Abdollahi *et al.*), *Phys. Rev. D*, **95** (2017) 082007.
[12] Fermi LAT Collaboration (Atwood W. *et al.*), *Astrophys. J.*, **697** (2009) 1071.
[13] Fermi Lat Collaboration (Abdo A. *et al.*), *Phys. Rev. Lett.*, **102** (2009) 181101.
[14] Fermi Lat Collaboration (Ackermann M. *et al.*), *Phys. Rev. D*, **82** (2010) 092003.
[15] Atwood W. *et al.*, arXiv:1303.3514.
[16] Smart D. F. and Shea M. A., *Adv. Space Res.*, **36** (2005) 2012.
[17] Finlay C. C. *et al.*, *Geophys. J. Int.*, **183** (2010) 12161010.
[18] Fermi LAT Collaboration (Ackermann M. *et al.*), *Astropart. Phys.*, **25** (2012) 346.
[19] Fermi LAT Collaboration (Ackermann M. *et al.*), *Astrophys. J. Suppl. Ser.*, **203** (2012) 4.
[20] AMS Collaboration (Aguilar M. *et al.*), *Phys. Rev. Lett.*, **113** (2014) 221102.
[21] H.E.S.S. Collaboration (Aharonian F. *et al.*), *Phys. Rev. Lett.*, **101** (2008) 261104.
[22] H.E.S.S. Collaboration (Aharonian F. *et al.*), *Astron. Astrophys.*, **508** (2009) 561.